Antimitotic Sulfonamides Inhibit Microtubule Assembly Dynamics and Cancer Cell Proliferation†

Renu Mohan,‡ Mithu Banerjee,§ Anasuya Ray,|| Tapas Manna,|| Leslie Wilson,|| Takashi Owa,⊥ Bhabatarak Bhattacharyya,§ and Dulal Panda*,‡

School of Biosciences and Bioengineering, Indian Institute of Technology Bombay, Mumbai 400076, India, Department of Biochemistry, Bose Institute, Centenary Campus, Kolkata 700054, India, Molecular, Cellular and Developmental Biology, University of California, Santa Barbara, and Laboratory of Seeds Finding Technology, Eisai Co., Ltd., 5-1-3 Tokodai, Tsukuba, Ibaraki 300-2635, Japan

Received November 16, 2005; Revised Manuscript Received March 15, 2006

ABSTRACT: Several sulfonamides have antitumor activities and are currently undergoing clinical evaluation for the treatment of cancer. In this study, we have elucidated the antiproliferative mechanism of action of five indole sulfonamides. The indole sulfonamides inhibited the polymerization of microtubule protein into microtubules in vitro. In addition, three representative derivatives, ER-68378 (**2**), ER-68384 (**4**) and ER-68394 (**5**), suppressed the dynamic instability behavior at the plus ends of individual steady-state microtubules in vitro. The analogues inhibited HeLa cell proliferation with half-maximal inhibitory concentrations in the range of 6−17 μM. The compounds blocked cell cycle progression at mitosis. At their lowest effective antimitotic concentrations, they depolymerized the spindle microtubules and disorganized the chromosomes but did not affect the microtubules in interphase cells. However, at relatively high concentrations, interphase microtubules were also depolymerized by these sulfonamides. Furthermore, all five compounds were found to induce apoptosis in the cells in association with the phosphorylation of bcl-2. The results suggest that the indole sulfonamides inhibit cell proliferation at mitosis by perturbing the assembly dynamics of spindle microtubules and that they can kill cancer cells by inducing apoptosis through the bcl-2-dependent pathway.

Sulfonamides, which have been clinically used for many years, have been found to possess a large number of different biological activities, including antibacterial, antiviral, antidiabetic, diuretic, and antithyroid activities (*1*−*4*). They exert their diverse pharmacological effects by interacting with a wide range of different cellular targets. For example, sulfonamides exert their antibacterial activity by targeting the folate biosynthetic pathway and act as diuretics by inhibiting carbonic anhydrase. Recently, sulfonamides have been used in retroviral therapy as HIV protease inhibitors (*5*−*7*). Using cell-based and micro array-based screening strategies, sulfonamide-focused compound libraries have also been evaluated for their antitumor potential (*8*−*11*). A structure−activity relationship study identified two classes of antitumor sulfonamides, represented by *N*-(3-chloro-7-indolyl)-1,4-benzenedisulfonamide (E7070) and *N*-[2-[(4-hydroxyphenyl)amino]-3-pyridinyl]-4-methoxybenzene sulfonamide (E7010). E7070 and its analogues belong to a novel class of cell cycle inhibitors that inhibit cell cycle progression at multiple checkpoints. These compounds exert antitumor properties by targeting the G1/S and/or G2/M phases of the cell cycle (*12*−*15*). Recently, E7010 (Figure 1) has been shown to block cells at mitosis by inhibiting tubulin polymerization (*16*, *17*). E7010 reversibly binds to the colchicine-binding site of β- tubulin, and it displays antitumor activity against both rodent tumors and several types of human tumor xenografts (*18*, *19*). In addition, the compound is also active against various types of drug-resistant tumor cell lines (*10*, *16*). Both E7070 and E7010 are currently undergoing phase II clinical evaluations and have demonstrated tolerable toxicity profiles and some objective antitumor responses (*20*−*24*).

Although E7010 and E7070 have been shown to inhibit tubulin polymerization (*10*) and cell proliferation, their antiproliferative mechanism of action is far from clear. Recently, a new class of indole sulfonamides was prepared with potential anticancer activity. In these derivatives, the amino substituted pyridine ring of E7010 was replaced by an indole group (*13*). Although all of the various sulfonamide analogues have been shown to bind to tubulin in a colchicine-competitive manner (*16*, *25*), a recent study has indicated that the mechanisms of action of the indole sulfonamides might differ from that of the earlier benzoyl derivatives (E7010) (*26*). For example, Nguyen et al. used docking studies to construct biochemically reasonable binding models for a diverse set of colchicine site inhibitors, thereby delineating the essential structural and functional features

† This work was supported by a grant from the Department of Biotechnology, Government of India (to D.P.), the Swarnajayanti Fellowship (to D.P.), U. S. Public Health Service Grant NS13560 (to L.W.), U.S. National Science Foundation Grant ITR 0331697 (to L.W and T.M.), and a CSIR grant from the Government of India (to B.B.).

* To whom correspondence should be addressed. Tel: 91-22-2576-7838. Fax: 91-22-2572-3480. E-mail: panda@iitb.ac.in.

‡ Indian Institute of Technology, Bombay.

§ Bose Institute.

|| University of California, Santa Barbara.

⊥ Eisai Co., Ltd.

10.1021/bi0523409 CCC: $33.50
Published on Web 04/07/2006

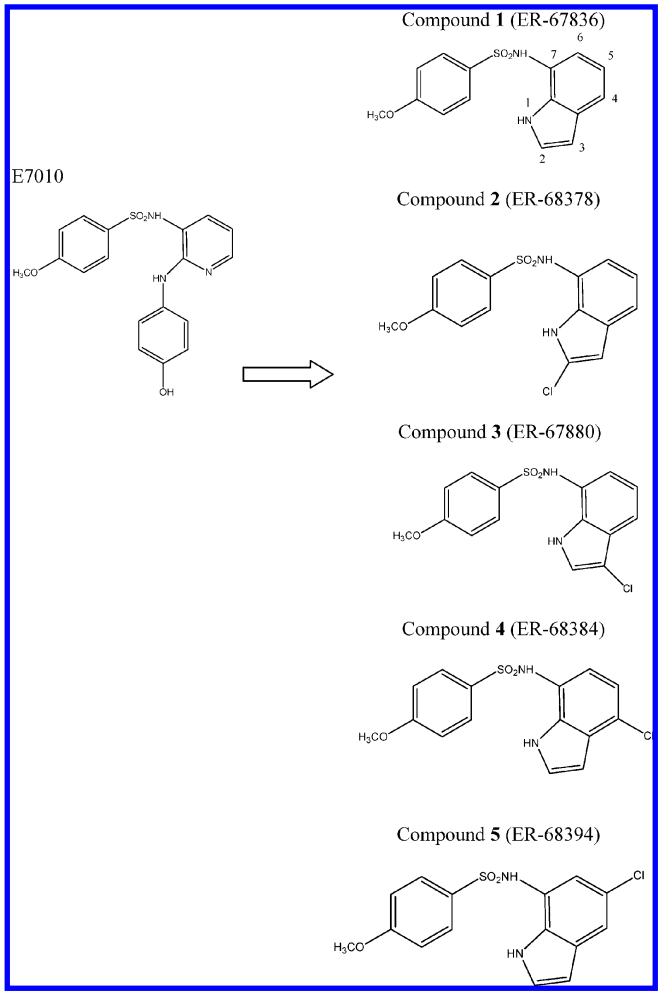

FIGURE 1: Chemical structures of E7010 and compounds **1**−**5**.

for inhibition (*26*). This docking study indicates that E7010 and the indole derivative (compound **3** in this work, see Figure 1) have distinct binding modes at the colchicine site of tubulin.

Tubulin heterodimers are the subunits of microtubules, dynamic cytoskeletal polymers that have many important cellular functions including the segregation of chromosomes to daughter cells during the processes of mitosis and cell division (*26*−*29*). The dynamic behaviors of spindle microtubules during mitosis are critical for the proper function of the spindle (*30*). It is well known that subtle suppression of microtubule dynamics by microtubule-targeted antimitotic drugs, such as the taxanes, the *vinca* alkaloids, and estramustine, prevents cell cycle progression in G2/M by inhibiting mitosis (*31*−*34*). In this work, we have examined the actions of five new indole sulfonamides (Figure 1) on proliferation and mitosis in HeLa cells and on microtubule polymerization and dynamics. The five derivatives differ from one another in the position of a single chlorine substituent, except for ER-67836 (**1**), which has no chlorine substituent. We have found that the five analogues inhibit cell cycle progression at mitosis by perturbing microtubule assembly dynamics. They also inhibited microtubule assembly both in vitro and in cells, and three of the derivatives that were examined, strongly suppressed the dynamic instability of individual microtubules in vitro. We also present evidence indicating that these sulfonamides induce apoptosis in association with the phosphorylation of bcl-2. Thus, the indole sulfonamides are promising candidates for the treatment of cancer.

EXPERIMENTAL PROCEDURES

Materials. Mouse monoclonal anti-α-tubulin antibody, mouse monoclonal anti-bcl-2 antibody, alkaline phosphatase conjugated anti-mouse IgG, 4, 6-diamidino-2-phenylindole (DAPI[11]), Hoechst 33258, BCIP/NBT, and fetal bovine serum were obtained from Sigma (St. Louis, MO). Mouse monoclonal anti-p53 (DO-1) antibody was purchased from Santa Cruz Biotechnology, California. Goat anti-mouse IgG-Alexa 568 conjugate was obtained from Molecular probes (Eugene, OR). All other reagents were of analytical grade. The five sulfonamide compounds tested in this study were synthesized and characterized spectroscopically, as previously published (*25*).

Cell Culture and Cell Proliferation Assays. HeLa cells were cultured in Eagle's minimal essential medium (Himedia) supplemented with 10% (v/v) fetal bovine serum, 1.5 g/L of sodium bicarbonate, and 1% antibiotic antimycotic solution containing streptomycin, amphotericin B, and penicillin. The cells were maintained at 37 °C in a humidified atmosphere of 5% carbon dioxide and 95% air. The cells were seeded at a density of 1×10^5 cells/mL on 96-well plates, and the inhibition of cell proliferation was determined using a standard sulforhodamine B assay as described previously (*35*). The cells were incubated with different concentrations of the five sulfonamides for one cell cycle (24 h). DMSO was used as a vehicle control. The cells were stained with 0.4% sulforhodamine B, and the concentration of the protein-bound dye was detected by measuring the absorbance at 560 nm.

Mitotic Index. HeLa cells (6×10^4 cells/mL) were grown on poly-L-lysine coated cover slips in 24-well tissue culture plates and treated with various concentrations of sulfonamides as described above. The cells were sedimented onto coverslips using a Labofuge 400R cytospin centrifuge (Heraeus, Germany) (1000*g*). The cells were fixed in 3.7% formaldehyde for 30 min at 37 °C and permeabilized with ice-cold methanol for 20 min. After washing with phosphate buffered saline (PBS), the cells were incubated with 1 μg/mL of 4,6-diamidino-2-phenylindole (DAPI) for 20 s at room temperature. Coverslips were mounted in 50% glycerol in PBS containing 1 mg/mL of ascorbic acid, and the cells were examined with a Nikon eclipse 2000-U fluorescence microscope using a 40× objective. Images were analyzed with Image Pro Plus software. The mitotic index was calculated as the percentage of mitotic cells in 500 cells counted per experiment.

Immunofluorescence Microscopy. Immunofluorescence microscopy was performed as described previously (*36*). Briefly, the cells were grown on coverslips and incubated with different concentrations of sulfonamides for one cell cycle (24 h). The cells were fixed and permeabilized as described previously (*36*, *37*). After blocking nonspecific

[1] Abbreviations: DAPI, 6-diamidino-2-phenylindole; PIPES, piperazine-*N*,*N*′-bis(2-ethanesulphonic acid); EGTA, ethylene glycol-bis-(2-aminoethyl ether)-*N*,*N*,*N*′,*N*′-tetraacetic acid; $MgCl_2$, magnesium chloride; GTP, guanosine 5′-triphosphate; PBS, phosphate buffered saline; EDTA, ethylenediaminetetraacetic acid; DTT, dithiothreitol; PMSF, phenylmethanesulfonyl fluoride.

sites with 2% BSA/PBS, the cells were incubated with the mouse monoclonal anti-α-tubulin antibody (1:300 dilution in 2% BSA/PBS) for 2 h at 37 °C followed by the Alexa-568 conjugated anti-mouse IgG antibody (1:100 dilution in 2% BSA/PBS) for 1 h at 37 °C. To observe p53 localization, the cells were stained with the mouse monoclonal anti-p53 antibody (1:250 dilution in 5% goat serum) for 1 h at 37 °C, followed by the Alexa conjugated secondary antibody. To visualize nuclei, the cells were incubated with DAPI and examined with a Nikon eclipse 2000-U fluorescence microscope as described earlier.

Determination of Apoptotic Cell Death. The cells seeded at a density of 1×10^5 cells/mL were incubated with different concentrations of sulfonamides. The cells were fixed and permeabilized as described earlier. After washing with PBS, 300 μL of Hoechst 33258 (2 μg/mL) was added to each well, and the wells were incubated in the dark at room temperature for 20 min. The cover slips were washed with PBS, mounted, and visualized by a fluorescence microscope.

Microtubule Protein Polymerization Assay. Microtubule protein (MTP) from a goat brain was prepared by two cycles of assembly and disassembly in a PEM buffer (50 mM PIPES, 1 mM EGTA, and 0.5 mM $MgCl_2$ at pH 6.9). The reaction mixture containing 15 μM of microtubule protein and the desired concentrations of sulfonamides were polymerized in a PEM buffer containing 1 mM GTP. The turbidity in the absence and presence of various concentrations of sulfonamides after 20 min at which polymerization reached the steady state were noted, and considering the turbidity for control samples as 100%, the percent inhibition of polymerization in the presence of different concentrations of sulfonamides were calculated. Fifty percent inhibition of polymerization (IC_{50}) for each of the compounds was determined by plotting the data points for the inhibition of polymerization vs the concentrations of the compounds.

Analysis of Microtubule Dynamic Instability. Purified tubulin (20 μM) was polymerized for 30 min at the ends of sea urchin (*Strongylocentrotus purpuratus*) axonemal seeds at 30 °C in the absence or presence of sulfonamides **2**, **4**, or **5** in 87 mM Pipes, 36 mM MES, 1.4 mM $MgCl_2$, and 1 mM EGTA at pH 6.8. The dynamic instability at the plus ends of individual microtubules was recorded (*35*). The ends were designated as either plus or minus on the basis of the growth rate, the number of microtubules that grew at opposite ends of the seeds, and the relative lengths of the microtubules. The changes in microtubule length with time were analyzed. Analysis started 30 min after polymerization initiation, when steady-state had been reached (*37*). Data points were collected at 3 to 5 s intervals. A microtubule was considered to be in a growth phase if it increased in length by >0.2 μm at a rate of > 0.3 μm/min. Microtubules showing length changes ≤ 0.2 μm over the duration of six data points were considered to be in an attenuated state.

Western Blot Analysis. HeLa cells were seeded at a density of 1×10^5 cells/mL in culture flasks. After incubating in the absence and presence of 25 μM each of compounds **1**, **2**, **3**, **4**, and **5** for one cell cycle (24 h) or 10 and 20 μM of compound **4**, the cells were harvested by using a cell scraper and centrifuged at 600*g* for 10 min. Cell lysates were prepared by lysing cell pellets in a lysis buffer (50 mM Tris, pH 7.4, 150 mM NaCl, 0.1% Triton X 100, 4 mM EDTA, 1 mM DTT, 1 mM PMSF, 50 mM NaF, and 0.2% Nonidet P-40) containing protease inhibitors followed by centrifugation at 750*g* for 20 min at 4 °C. The protein concentration of the extract was determined by the Bradford assay. Equal quantities of protein (50 μg) were separated by 10% SDS−PAGE and blotted onto a nitrocellulose membrane (Pall Corporation). The membrane was probed with the mouse monoclonal anti-bcl-2 antibody (1:1000 dilution in Tris buffered saline containing 0.1% Triton X 100) for 2 h at room temperature. Bound antibodies were detected with anti-mouse IgG-alkaline phosphatase conjugate (1:5000 dilution) for 1 h. After washing, the blot was developed using the BCIP/NBT substrate.

RESULTS

Effects of Indole Sulfonamides on Microtubule Polymerization In Vitro. The effects of the five indole sulfonamides (compounds **1**−**5**) on microtubule polymerization in vitro were analyzed using bovine brain MAP-rich microtubule protein (70% tubulin and 30% MAPs). As shown in Figure 2, all five analogues inhibited the rate and extent of polymerization in a concentration-dependent manner. The concentrations required for half-maximal inhibition of polymerization were 20, 10, 24, 25, and 15 μM for sulfonamides **1**−**5**, respectively. Although all five analogues were generally similar in potency, compounds **2** and **5** were more potent than the others.

Effects of Indole Sulfonamide Compounds on Dynamic Instability of Individual Microtubules In Vitro at Steady State. The effects of three of the analogues, compounds **2**, **4**, and **5**, on the dynamic instability parameters of individual microtubules at their plus ends at steady state are shown in Table 1. All three compounds strongly decreased the shortening rate, the fraction of time the microtubules spent growing, and the overall dynamicity while increasing the fraction of time the microtubules spent in an attenuated (paused) state. For example, 0.5 μM compound **5** reduced the shortening rate by 66% and the percentage of time spent growing by 75%, and it suppressed the overall dynamicity by 76%. In addition, the three sulfonamides reduced the catastrophe and rescue frequencies. For example, 0.5 μM compound **5** reduced the catastrophe frequency by 54%. Under the same conditions, compounds **2**, **4**, and **5** had no detectable effects on the microtubule polymer mass (data not shown), revealing that their effects on dynamic instability are much stronger than their effects on polymer mass.

Effect of the Indole Sulfonamides on HeLa Cell Proliferation. The effects of compounds **1**−**5** on the proliferation of human cervical cancer (HeLa) cells were determined by incubating the cells with different concentrations (0.1 to 20 μM) of the compounds for 24 h. All of the sulfonamides produced a concentration-dependent inhibition of cell proliferation. The concentrations required to produce the half-maximal inhibition of proliferation (IC_{50}) varied in a narrow range from 6 to 17 μM, as shown in Table 2. Compound **4** was the most potent with an IC_{50} of 6 ± 1 μM.

Indole Sulfonamides Blocked Cell Cycle Progression at Mitosis. Inhibitors of microtubule assembly dynamics, including vinblastine, taxol, colchicine, and griseofulvin, have been shown to inhibit cell proliferation by blocking cell cycle progression at mitosis (*27*). Therefore, the effects of the five sulfonamides on cell cycle progression were examined. All

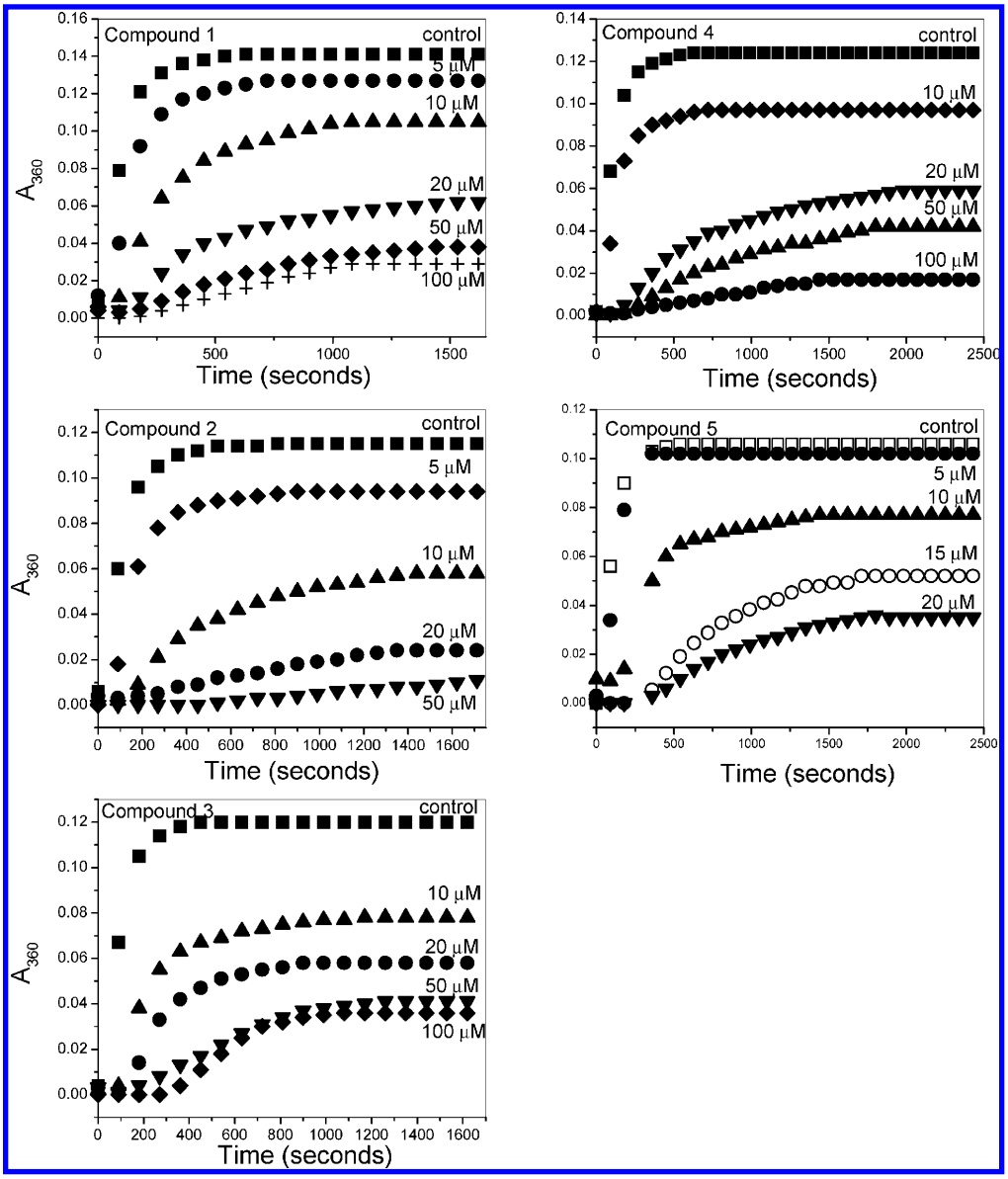

FIGURE 2: Inhibition of microtubule polymerization by compounds **1**−**5**. The polymerization of microtubule protein (15 μM) was measured in the absence and presence of different concentrations of the sulfonamides. The effects of compounds **1**−**5** on microtubule assembly were monitored by measuring the increase in the turbidity at 360 nm with time as described in Experimental Procedures.

Table 1: Suppression of Steady State In Vitro Microtubule Dynamics at the Plus Ends by Sulfonamides **2**, **4**, and **5**[a]

	control	compd **2** (2.5 μM)	compd **4** (2.5 μM)	compd **5** (0.5 μM)
growth rate (μm/min)	1.7 ± 0.8 (11)	1.7 ± 0.6 (10)	2.3 ± 1.1 (8)	1.8 ± 0.5 (12)
shortening rate (μm/min)	28.4 ± 7.3 (24)	6.9 ± 3.70 (20)	15.6 ± 8.1 (20)	9.5 ± 3.3 (24)
growing length (μm)	2.3 ± 0.7	1.7 ± 0.6	2 ± 0.09	1.9 ± 0.4
shortening length (μm)	5.0 ± 2.3	3.1 ± 0.4	5.0 ± 0.5	3.5 ± 0.9
% time growing	44.8%	10.2%	7.6%	11.0%
% time shortening	7.7%	10.3%	7.5%	9.3%
%time attenuated	47.1%	79.5%	84.9%	79.8%
catastrophe frequency (per min)	0.48 ± 0.07	0.23 ± 0.05	0.2 ± 0.05	0.22 ± 0.05
rescue frequency (per min)	1.8 ± 0.7	1.01 ± 0.3	1.01 ± 0.4	1.10 ± 0.3
dynamicity	2.3	0.5	0.7	0.55

[a] Growth rate, shortening rate, and growing and shortening lengths are in ± SD. Catastrophe and rescue frequencies are in ± SEM. Tubulin concentration is 20 μM.

five sulfonamides inhibited mitosis in a concentration-dependent manner. For example, 26 and 57% of the cells were arrested at mitosis by 3 and 6 μM compound **4**, respectively (Figure 3). The induction of mitotic block occurred in parallel with the inhibition of cell proliferation. For example, 6 μM compound **4** inhibited HeLa cell proliferation by 50%, and it arrested mitosis by 57%. The concentrations that produced 50% arrest at mitosis (MB_{50}) were 19 ± 4, 10 ± 1, 15 ± 3, 6 ± 2, and 15 ± 1 for compounds **1**, **2**, **3**, **4**, and **5**, respectively. The results indicate

Table 2: Effects of Sulfonamide Analogues on the Proliferation and Cell Cycle Progression of HeLa Cells[a]

compd	sulfonamides	chemical formula	IC_{50} (μM)	MB_{50} (μM)
1	(ER-67836)	$C_{15}H_{14}N_2O_3S$	17 ± 1	19 ± 4
2	(ER-68378)	$C_{15}H_{13}N_2O_3SCl$	10 ± 2	10 ± 1
3	(ER-67880)	$C_{15}H_{13}N_2O_3SCl$	15 ± 2	15 ± 3
4	(ER-68384)	$C_{15}H_{13}N_2O_3SCl$	6 ± 1	6 ± 2
5	(ER-68394)	$C_{15}H_{13}N_2O_3SCl$	13 ± 2	15 ± 1

[a] IC_{50} represents half-maximal inhibitory concentration for HeLa cell proliferation. MB_{50} represents concentration of compounds that produce 50% of the cells to be arrested in mitosis. Data are the average of three independent experiments, presented together with ± S. D. Each individual experiment was performed in duplicate.

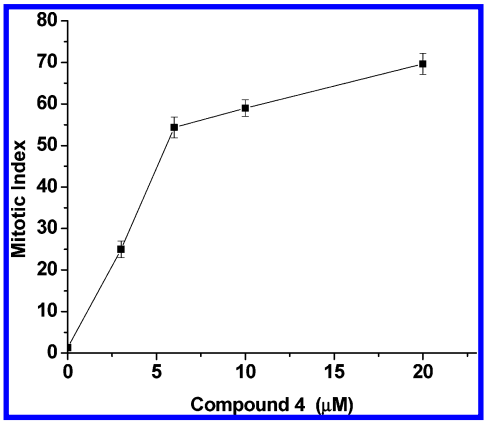

FIGURE 3: Effects of compound **4** on the mitotic index in HeLa cells. The mitotic index was determined by DAPI staining as described in Experimental Procedures.

that all of the indole sulfonamides inhibit HeLa cell proliferation by blocking the cells at mitosis.

Effect of Indole Sulfonamides on Mitotic Spindle Organization. All five of the indole sulfonamides perturbed HeLa cell spindle organization. As shown in Figure 4A, the metaphase spindles of untreated cells were bipolar with their chromosomes organized into a compact metaphase plate. In a manner typical of all five analogues, compound **4** severely perturbed mitotic spindle organization. For example, at 6 μM compound **4**, ~60% of the cells displayed abnormal spindle organization. Many of the cells had multipolar spindles, whereas others had aberrant bipolar spindles with misaligned chromosomes (Figure 4B). The chromosomes in some of the cells remained at the poles. The chromosomes in most cells were organized into condensed ball shaped arrays (Figure 4C). Multipolar spindles, abnormal bipolar spindles, and ball shaped chromosomes were also found at 10 and 20 μM concentrations of this compound (Figure 4C). The spindle microtubules in cells treated with 6 μM compound **4** were significantly depolymerized (Figure 4B). At 20 μM compound **4**, the spindle microtubules were significantly shorter in length than the control microtubules (Figure 4A and C). At a concentration of 10 μM, compounds **1**, **2**, and **3** (Figure 4 D, F, and H) and compound **1** at 20 μM concentration (Figure 4E), short multipolar spindles and tubulin aggregates were found. At 20 μM compounds **2** and **3** (Figure 4G and I) and 10 μM compound **5** (Figure 4J), the spindle microtubules were completely depolymerized, and only tubulin aggregates were found. The chromosomes were organized into ball shaped contracted, globular masses (Figure 4E−J).

Effect of Indole Sulfonamides on Interphase Microtubules. The effects of the indole sulfonamides were also analyzed on interphase microtubules. All five of the indole sulfonamides depolymerized the interphase microtubules in a concentration-dependent manner, but depolymerization of interphase microtubules required higher sulfonamide concentrations than those required to disrupt the spindle microtubules (Figure 5 B−V). For example, at its half-maximal inhibitory concentration for blocking mitosis with compound **4** (6 μM), the organization and density of the interphase microtubules were similar to those of control cells (Figure 5N). Higher concentrations of compound **4** depolymerized the interphase microtubules (Figure 5O, Q, R). Furthermore, high concentrations of compound **4** (10 and 20 μM) also induced multinucleation (Figure 5P). At 10 μM compound **4**, 40% of the interphase cells contained 2−4 nuclei/cell. At 50 μM compound **4**, the interphase microtubules were completely absent, and only tubulin aggregates remained. Similar results were obtained with compounds **1**, **2**, **3**, and **5** (Figure 5C−I, K−M, and T−V).

The Indole Sulfonamides Induced Bcl-2 Phosphorylation. It was previously shown that microtubule-targeted agents that block cell cycle progression at mitosis also induce apoptotic cell death (*38*). Thus, we determined whether the indole sulfonamides could induce apoptosis. HeLa cells were treated with either the vehicle or different concentrations of sulfonamides for 24 h. As shown in Figure 6 with compound **4**, a representative sulfonamide, Hoechst 33258 staining of the chromatin showed the characteristics of apoptotic cell death, including nuclear envelope blebbing and nuclear condensation, indicating that compound **4** indeed induces apoptotic cell death (Figure 6B) (*39*) Similar results were obtained with the other tested sulfonamides (data not shown). Several microtubule-targeted agents that induce apoptosis are also known to hyperphosphorylate bcl-2, and it has been suggested that hyperphosphorylation of bcl-2 induces apoptotic cell death (*40*, *41*). The levels of bcl-2 phosphorylation in the cells treated with the vehicle and 10 or 20 μM compound **4** were examined using anti-bcl-2 antibody (Figure 6C). The vehicle-treated cells showed no phosphorylation, whereas the compound **4**-treated cells showed significant phosphorylation of bcl-2. (Figure 6C, lanes 2 and 3). Similarly, the other indole sulfonamides also induced bcl-2 phosphorylation (Figure 7). Thus, like several other microtubule-targeted antimitotic agents, sulfonamides induce apoptosis by hyperphosphorylating bcl-2.

Another major mechanism of apoptotic cell death is driven by the activation of p53 (*42*). To examine whether p53 is involved in apoptosis caused by compound **4**, the nuclear accumulation of p53 protein was studied. Immunofluorescence studies performed with anti-p53 antibody showed no difference in the nuclear concentration of p53, both in the untreated and sulfonamide-treated cells, indicating that compound **4** does not induce apoptosis by the p53 pathway (data not shown).

DISCUSSION

Five different sulfonamides, **1**−**5**, containing an indole scaffold were found to inhibit HeLa cell proliferation with half-maximal inhibitory concentrations ranging from 6 to 17 μM. Of the five compounds examined, compound **4** was the

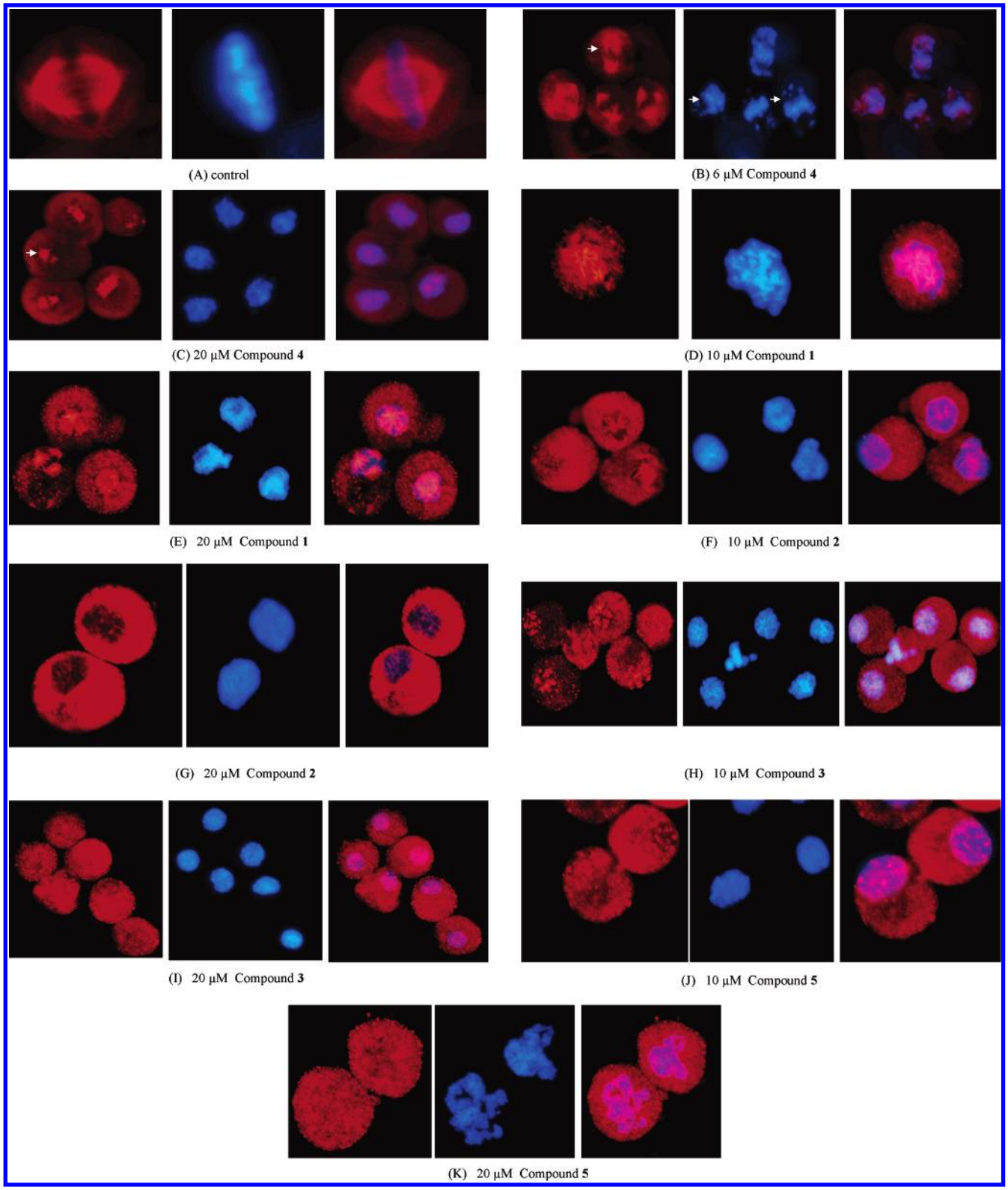

FIGURE 4: Effects of sulfonamides **1**−**5** on spindle microtubules and chromosome organization of HeLa cells. The cells were incubated in the absence (A) and presence of 6 μM (B) and 20 μM (C) compound **4**; 10 μM compound **1** (D), 20 μM compound **1** (E); 10 μM compound **2** (F), 20 μM compound **2** (G); 10 μM compound **3** (H), 20 μM compound **3** (I); 10 μM compound **5** (J); and 20 μM compound **5** (K) for 24 h. The spindle microtubules (red) and chromosomes (blue) were analyzed as described in Experimental Procedures.

most potent with an IC_{50} of 6 ± 1 μM. The inhibition of proliferation occurred together with the induction of apoptosis in association with the phosphorylation of bcl-2. The antimitotic activities of the indole sulfonamides paralleled their abilities to inhibit cell proliferation. The indole sulfonamides induced depolymerization both of interphase and mitotic spindle microtubules, with the effects on spindle microtubules being much stronger than those on interphase microtubules (see below). All of the compounds inhibited the polymerization of purified microtubule protein into microtubules with moderate potencies in vitro. The effects of three representative sulfonamides (compounds **2**, **4**, and

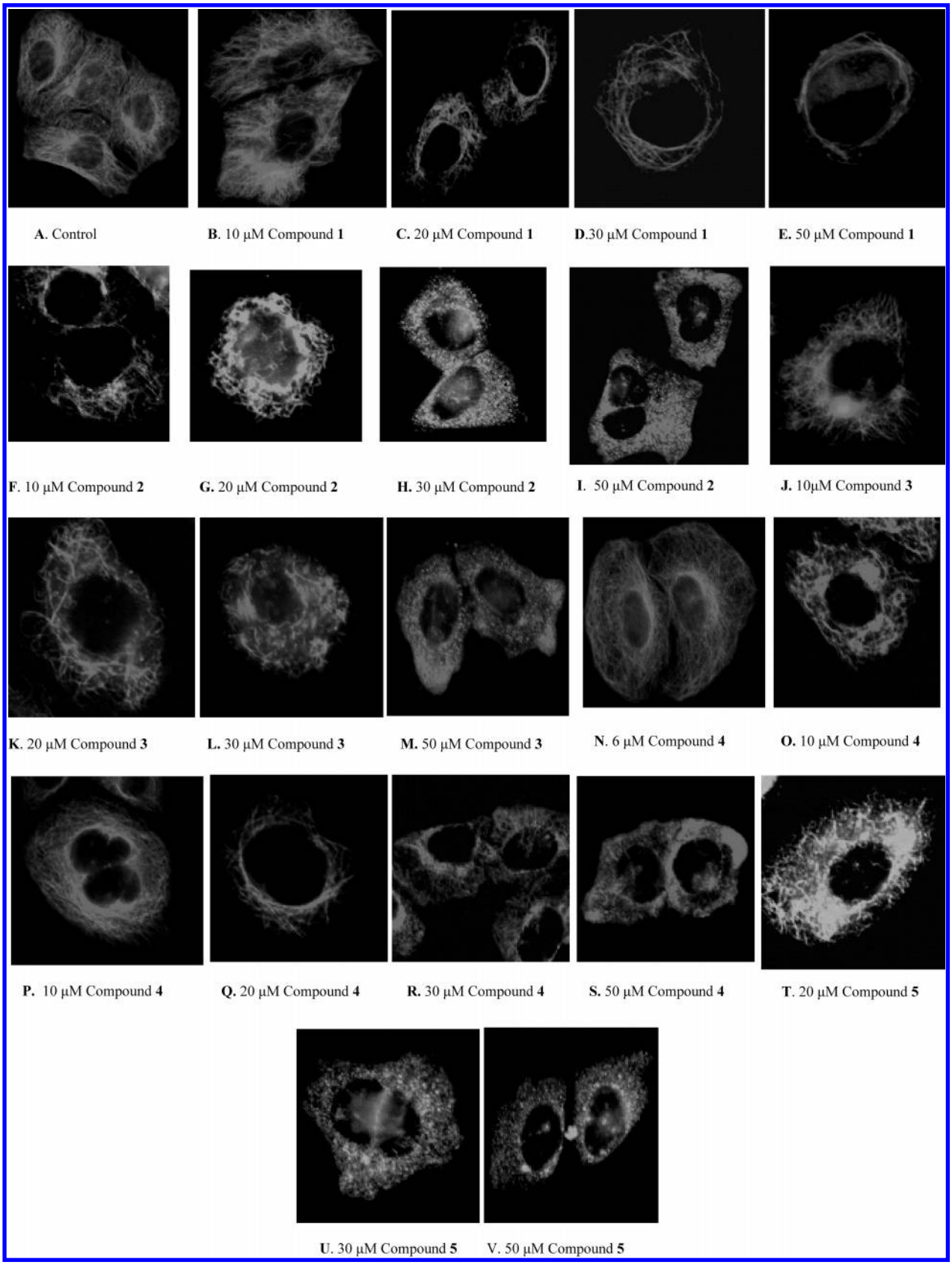

FIGURE 5: Effects of sulfonamides **1**−**5** on the interphase microtubules of HeLa cells. The cells were incubated with the vehicle (A), 10 μM (B), 20 μM (C), 30μM (D), and 50 μM (E) compound **1**; 10 μM (F), 20 μM (G), 30μM (H), and 50 μM (I) compound **2**; 10 μM (J), 20 μM (K), 30μM (L), and 50 μM (M) compound **3**; 6 μM (N), 10 μM (O, P), 20 μM (Q), 30μM (R), and 50 μM (S) compound **4**; 20 μM (T), 30μM (U), and 50 μM (V) compound **5** for 24 h and stained with the α-tubulin antibody.

5) on the steady-state dynamic instability behavior of individual microtubules at their plus ends in vitro were found to be much stronger than their effects on the polymer mass. All three drugs suppressed growing and shortening dynamics, with the strongest suppressive effects on the rate and extent of shortening and the fraction of time the microtubules spent

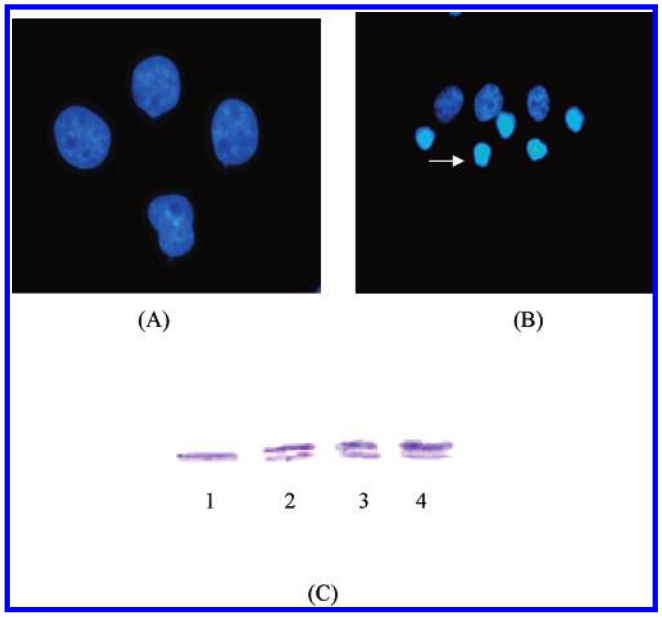

FIGURE 6: Induction of apoptosis in HeLa cells by compound **4**. The HeLa cells were grown in the absence (A) and presence of compound **4** (20 μM) (B). The chromosomes were stained with Hoechst 33258. The effects of compound **4** on the phosphorylation state of bcl-2 (C). Western blot of a HeLa cell lysate treated with the vehicle (lane 1), 10 μM compound **4** (lane 2), 20 μM compound **4** (lane 3), and 100 nM taxol (lane 4).

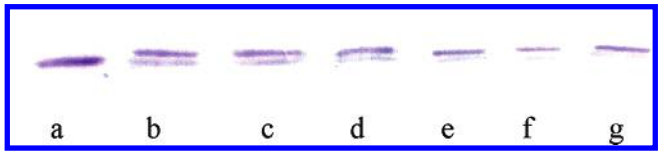

FIGURE 7: Effect of compounds **1**−**5** on the phosphorylation state of bcl-2. Western blot of a HeLa cell lysate treated with the vehicle (a), 25 μM each of compound **1** (b), compound **2** (c), compound **3** (d), compound **4** (e), and compound **5** (f) and 100 nM taxol (g).

in the growing phase (Table 1). These activities are consistent with those of several other known antimitotic agents, such as vinblastine, colchicine, cryptophycin-52, griseofulvin, and benomyl (*27*, *34*, *36*, *37*). The results together suggest that the indole sulfonamides inhibit HeLa cell proliferation at mitosis by suppressing spindle microtubule dynamics.

Possible Mechanisms by which the Indole Sulfonamides Might Suppress Plus-End Dynamic Instability. Using K_a values from a previous study on the binding of the indole sulfonamides to tubulin (*25*), in a suspension containing 20 μM tubulin and the drug concentrations used in Table 1 (2.5, 2.5, and 0.5 μM of compounds **2**, **4**, and **5**, respectively) we calculated that only 10.5, 7.5, and 2.3% of the soluble tubulin would have been bound to tubulin under the conditions used. Thus, a relatively small number of drug molecules bound to soluble tubulin appears to be sufficient to produce large effects on the suppression of dynamics. These results suggest that the suppression of dynamics is probably brought about by the binding of free sulfonamide molecules or sulfonamide−tubulin complexes at the ends. The binding of a few molecules of free sulfonamides or sulfonamide−tubulin complexes to the tips or their incorporation into the microtubule lattice as sulfonamide−tubulin complexes could stabilize the ends against depolymerization and reduce the rate and extent of shortening as occurs with colchicine−tubulin complexes (*43*). The presence of the compounds at the microtubule ends or their incorporation into the microtubule lattice, as occurs with colchicine, may also be responsible for preventing microtubule growth, either by sterically blocking further addition of tubulin dimers to the ends or by perturbing the ends. A microtubule could resume growth by dissociation of the bound sulfonamide.

Inhibition of Mitosis by the Indole Sulfonamides. The assembly dynamics of spindle microtubules are crucial for chromosome segregation during mitosis, and it is believed that at their lowest effective concentrations, many antimitotic drugs inhibit mitosis at the metaphase/anaphase transition, primarily by suppressing microtubule dynamics (*27*, *30*, *31*, *36*, *37*). The indole sulfonamides depolymerized both interphase and spindle microtubules; however, they had a stronger depolymerizing effect on spindle microtubules than on interphase microtubules. This may occur because spindle microtubules are more dynamic than interphase microtubules, and their stability is regulated differently than that in interphase microtubules (*27*). Similar differential depolymerization activity has been observed for several agents that inhibit mitosis by targeting microtubules (*31*, *34*, *36*, *37*).

At relatively high concentrations (10−20 μM), compound **4** induced the formation of multinucleated cells, which are thought to arise when cells exit mitosis without cytokinesis and undergo multiple rounds of DNA replication (*44*, *45*). Nuclear division without cytokinesis results in polyploidy (*46*). Owa et al. found that compound **4** induced the formation of 4 and 8N peaks in p388 cells as determined by flow cytometry (*11*). The results suggest that relatively high concentrations of compound **4** induce abnormal mitosis leading to polyploidy and multinucleation in certain tumor cells.

The indole sulfonamides killed HeLa cells by inducing apoptosis (Figure 6). Western blot analysis of the lysates of cells treated with compounds **1**−**5** showed an increase in bcl-2 phosphorylation (Figure 6C and Figure 7), suggesting the involvement of this apoptotic pathway. The bcl-2 family plays a key role in apoptotic regulation with some members (bax and bad) promoting apoptosis and others (bcl-2 and bcl-x_l) promoting cell survival (*47*, *48*). Competitive dimerization between bcl-2 family members regulates the activation of caspases leading to nuclear disintegration and cell death. For example, heterodimerization of bcl-2 and bax prevents bax-mediated apoptosis. Bcl-2 function is regulated through phosphorylation (*49*). Several microtubule targeting compounds are known to induce phosphorylation at serine-70 and serine-87 residues of bcl-2 (*50*, *51*). The phosphorylation leads to the loss of anti-apoptotic function of bcl-2, by decreasing its ability to heterodimerize with bax and, thus, promotes apoptosis. Thus, similar to other microtubule interacting drugs, the indole sulfonamides appear to induce apoptosis in association with the phosphorylation of bcl-2.

The cells treated with compound **4** showed no increase in the nuclear concentration of p53 (data not shown). This finding rules out the possibility of p53-mediated apoptosis in these cells (*52*, *53*). Many of the microtubule interacting agents such as taxol and vinblastine do not induce p53 accumulation, whereas DNA damaging agents induce p53 nuclear accumulation. Recent studies have shown that colchicine- and taxol-triggered mitotic block induces p53-independent apoptosis (*54*, *55*).

A number of antimitotic sulfonamides have entered clinical trials as potential anticancer agents (*22*−*24*). The results

obtained herein indicate that the antimitotic indole sulfonamides inhibit cancer cell proliferation at mitosis and induce apoptosis in a fashion similar to that of known microtubule-targeting agents such as taxol and vinblastine. Furthermore, unlike taxol and vinblastine, E7010 and the indole sulfonamides have been shown to exhibit good growth inhibitory activity against P-glycoprotein overexpressing MDR cell lines such as the human colon cancer lines HCT15 and DLD-1 (ref *16* and unpublished data by T. O.). Although the antitumor efficacy of the indole sulfonamides has not yet been evaluated in animal models, our results indicate that these compounds may serve as important lead compounds for the development of novel anticancer drugs.

ACKNOWLEDGMENT

Renu Mohan thanks the University Grant Commission of the Government of India for a Fellowship. We thank K. Rathinasamy and Dipti Rai for the critical reading of the manuscript.

REFERENCES

1. Maren, T. H., and Conroy, C. W. (1993) A new class of carbonic anhydrase inhibitor, *J Biol. Chem. 268*, 26233−26239.
2. Scozzafava, A., Owa, T., Mastrolorenzo, A., and Supuran, C. T. (2003) Anticancer and antiviral sulfonamides, *Curr. Med. Chem. 10*, 925−953.
3. Owa, T., Yoshino, H., Okauchi, T., Yoshimatsu, K., Ozawa, Y., Sugi, N. H., Nagasu, T., Koyanagi, N., and Kitoh, K. (1999) Discovery of novel antitumor sulfonamides targeting G1 phase of the cell cycle, *J. Med. Chem. 42*, 3789−3799.
4. Koyanagi, N., Nagasu, T., Fujita, F., Watanabe, T., Tsukahara, K., Funahashi, Y., Fujita, M., Taguchi, T., Yoshino, H., and Kitoh, K. (1994) *In vivo* tumor growth inhibition produced by a novel sulfonamide, E7010, against rodent and human tumors, *Cancer Res. 54*, 1702−1706.
5. Ghosh, K. A., Swanson, M. L., Cho, H., Leschenko, S., Hussain, A. K., Kays, S., Walker, E. D., Koh, Y., and Mitsuya, H. (2005) Structure-based design: Synthesis and biological evaluation of a series of novel cyclo-amide derived HIV-1 protease inhibitors, *J. Med. Chem. 48*, 3576−3585.
6. Yeung, M. C., Klein, L. L., Flentge, A. C., Randolph, T. J., Zhao, C., Ming, H. S., Tatyana, D., Vincent, S. S., and Kempf, J. D. (2005) Oximinosulfonamides as potent HIV protease inhibitors, *Bioorg. Med. Chem. Lett. 15*, 2275−2278.
7. Fung, B. H., Kisrchenbaum, L. H., and Hameed, R. (2000) Amprenavir: A new human immunodeficiency virus type1 protease inhibitor, *Clin. Ther. 22*, 549−572.
8. Yokoi, A., Kuromitsu, J., Kawai, T., Nagasu, T., Sugi, N. H., Yoshimatsu, K., Yoshino, H., and Owa, T. (2002) Profiling novel sulfonamide antitumor agents with cell-based phenotypic screens and array-based gene expression analysis, *Mol. Cancer Ther. 1*, 275−286.
9. Oda, Y., Owa, T., Sato, T., Boucher, B., Daniels, S., Yamanaka, H., Shinohara, Y., Yokoi, A., Kuromitsu, J., and Nagasu, T. (2003) Quantitative chemical proteomics for identifying candidate drug targets, *Anal. Chem. 75*, 2159−2165.
10. Owa, T., Yokoi, A., Yamazaki, K., Yoshimatsu, K., Yamori, T., and Nagasu, T. (2002) Array-based structure and gene expression relationship study of antitumor sulfonamides including [2-[(4-hydroxyphenyl)amino]-3-pyridinyl]-4-methoxybenzenesulfonamide and *N*-(3-chloro-7-indolyl)-1,4-benzenedisulfonamide, *J. Med. Chem. 45*, 4913−4922.
11. Owa, T., Okauchi, T., Yoshimatsu, K., Sugi, N. H., Ozawa, Y., Nagasu, T., Koyanagi, N., Okabe, T., Kitoh, K., and Yoshino, H. (2000) A focused compound library of novel N-(7-indolyl)-benzenesulfonamides for the discovery of potent cell cycle inhibitors, *Bioorg. Med. Chem. Lett. 10*, 1223−1226.
12. Ozawa, Y., Sugi, N. H., Nagasu, T., Owa, T., Watanabe, T., Koyanagi, N., Yoshino, H., Kitoh, K., and Yoshimatsu, K. (2001) E7070, a novel sulphonamide agent with potent antitumour activity *in vitro* and *in vivo*, *Eur. J. Cancer. 37*, 2275−2282.
13. Owa, T., Yoshino, H., Yoshimatsu, K., and Nagasu, T. (2001) Cell cycle regulation in the G1 phase: a promising target for the development of new chemotherapeutic anticancer agents, *Curr. Med. Chem. 8*, 1487−1503.
14. Fukuoka, K., Usuda, J., Iwamoto, Y., Fukumoto, H., Nakamura, T., Yoneda, T., Narita, N., Saijo, N., and Nishio, K. (2001) Mechanisms of action of the novel sulfonamide anticancer agent E7070 on cell cycle progression in human non-small cell lung cancer cells, *Invest. New Drugs 19*, 219−227.
15. Laconde, G., Pommery, N., Depreux, P., Berthelot, P., and Henichart, J. P. (2003) New analogues of the anticancer E7070: synthesis and pharmacology, *J. Enzyme Inhib. Med. Chem. 18*, 89−94.
16. Yoshimatsu, K., Yamaguchi, A., Yoshino, H., Koyanagi, N., and Kitoh, K. (1997) Mechanism of action of E7010, an orally active sulfonamide antitumor agent: inhibition of mitosis by binding to the colchicine site of tubulin, *Cancer Res. 57*, 3208−3213.
17. Gwaltney, S. L., II, Imade, H. M., Li, Q., Gehrke, L., Credo, R. B., Warner, R. B., Lee, J. Y., Kovar, P., Frost, D., Ng, S. C., and Sham, H. L. (2001) Novel sulfonate derivatives: potent antimitotic agents, *Bioorg. Med. Chem. Lett. 11*, 1671−1673.
18. Iwamoto, Y., Nishio, K., Fukumoto, H., Yoshimatsu, K., Yamakido, M., and Saijo, N. (1998) Preferential binding of E7010 to murine beta 3-tubulin and decreased beta 3-tubulin in E7010-resistant cell lines, *Jpn. J. Cancer Res. 89*, 954−962.
19. Nihei, Y., Suzuki, M., Okano, A., Tsuji, T., Akiyama, Y., Tsuruo, T., Saito, S., Hori, K., and Sato, Y. (1999) Evaluation of antivascular and antimitotic effects of tubulin binding agents in solid tumor therapy, *Jpn. J. Cancer Res. 90*, 1387−1395.
20. Van Kesteren, C., Beijnen, J. H., and Schellens, J. H. (2002) E7070: a novel synthetic sulfonamide targeting the cell cycle progression for the treatment of cancer, *Anti-Cancer Drugs 13*, 989−997.
21. Funahashi, Y., Koyanagi, N., and Kitoh, K. (2001) Effect of E7010 on liver metastasis and life span of syngeneic C57BL/6 mice bearing orthotopically transplanted murine Colon 38 tumor, *Cancer Chemother. Pharmacol. 47*, 179−184.
22. Yamamoto, K., Noda, K., Yoshimura, A., Fukuoka, M., Furuse, K., and Niitani, H. (1998) Phase I study of E7010, *Cancer Chemother. Pharmacol. 42*, 127−134.
23. Smyth, J. F., Aamdal, S., Awada, A., Dittrich, C., Caponigro, F., Schoffski, P., Gore, M., Lesimple, T., Djurasinovic, N., Baron, B., Ravic, M., Fumoleau, P., and Punt, C. J. (2005) EORTC new drug development and melanoma groups. Phase II study of E7070 in patients with metastatic melanoma, *Ann. Oncol. 16*, 158−161.
24. Supuran, C. T. (2003) Indisulam: an anticancer sulfonamide in clinical development, *Expert Opin. Invest. Drugs 12*, 283−287.
25. Banerjee, M., Poddar, A., Mitra, A., Surolia, A., Owa, T., and Bhattacharya, B. (2005) Sulfonamide drugs binding to the colchicine site of tubulin: Thermodynamic analysis of the drug-tubulin interactions by isothermal titration calorimetry, *J. Med. Chem. 48*, 547−555.
26. Nguyen, T. L., McGrath, C., Hermone, A. R., Burnett, J. C., Zaharevitz, D. W., Day, B. W., Wipf, P., Hamel, E., and Gussio, R. (2005) A common pharmacophore for a diverse set of colchicine site inhibitors using a structure-based approach, *J. Med. Chem. 48*, 6107−6116.
27. Jordan, M. A., and Wilson, L. (2004) Microtubules as a target for anticancer drugs, *Nat. Rev. 4*, 253−265.
28. Lodish, H., Baltimore, D., Berk, A., Zipursky, S. L., Matsudaira, P., and Darnell, J. (1999) *Molecular Cell Biology*, W. H. Freeman, New York.
29. Nogales, E., Whittaker, M., Milligan, R. A., and Downing, K. H. (1999) High resolution model of the microtubule, *Cell 96*, 76−78.
30. Desai, A., and Mitchison, T. J. (1997) Microtubule polymerization dynamics, *Annu. Rev. Cell Biol. 13*, 83−117.
31. Wilson, L., Panda, D., and Jordan, M. A. (1999) Modulation of microtubule dynamics by drugs: A paradigm for the action of cellular regulators, *Cell Struct. Funct. 24*, 329−335.
32. Panda, D., Miller, H. P., Islam, K., and Wilson, L. (1997) Stabilization of microtubule dynamics by estramustine by binding to a novel site in tubulin: a possible mechanistic basis for its antitumor action, *Proc. Natl. Acad. Sci. U.S.A. 94*, 10560−10564.
33. Hamel, E. (1996) Antimitotic natural products and their interactions with tubulin, *Med. Res. Rev. 16*, 207−231.
34. Panda, D., DeLuca, K., Williams, D., Jordan, M. A., and Wilson, L. (1998) Antiproliferative mechanism of action of cryptophycin-

52: Kinetic stabilization of microtubule dynamics by high affinity binding to microtubule ends, *Proc. Natl. Acad. Sci. U.S.A. 95*, 9313−9318.
35. Skehan, P., Storeng, R., Scudiero, D., Monks, A., McMahon, J., Vistica, D., Warren, J. T., Bokesh, H., Kenney, S., and Boyd, M. R. (1990) New colorimetric cytotoxicity assay for anticancer drug screening, *J. Natl. Cancer Inst. 82*, 1107−1112.
36. Gupta, K., Bishop, J., Peck, A., Brown, J., Wilson, L., and Panda, D. (2004) Antimitotic antifungal compound benomyl inhibits brain microtubule polymerization and dynamics and cancer cell proliferation at mitosis, by binding to a novel site in tubulin, *Biochemistry 43*, 6645−6655.
37. Panda, D., Rathinasamy, K., Santra, M. K., and Wilson, L. (2005) Kinetic suppression of microtubule dynamic instability by griseofulvin: Implications for its possible use in the treatment of cancer, *Proc. Natl. Acad. Sci. U.S.A. 102*, 9878−9883.
38. Wang, L. G., Lui, X. M., Kruis, W., and Budman, D. R. (1999) The effect of antimicrotubule agents on the signal transduction pathways of apoptosis: A review, *Cancer Chemother. Pharmacol. 44*, 355−361.
39. Negri, L., Donzelli, M., Bernardi, R., Rossi, L., Burkle, A., and Scovassi, I. (1997) Multiparametric staining to identify apoptotic human cells, *Exp. Cell Res. 234*, 174−177.
40. Blagoskonny, M. V., Giannakakou, P., el-Deiry, W. S., Kingston, D. G., Higgs, P. I., Neckers, L., and Fojo, T. (1997) Raf-1/bcl-2 phosphorylation: a step from microtubule damage to cell death, *Cancer Res. 57*, 130−135.
41. Haldar, S., Jena, N., and Croce, C. M. (1995) Inactivation of bcl-2 by phosphorylation, *Proc. Natl. Acad. Sci. U.S.A. 92*, 4507−4511.
42. Khan, S. H., and Wahl, G. M. (1998) P53 and pRb prevent rereplication in response to microtubule inhibitors by mediating a reversible G1 arrest, *Cancer Res. 58*, 396−401.
43. Panda, D., Daijo, J. E., Jordan, M. A., and Wilson, L. (1995) Kinetic stabilization of microtubule dynamics at steady state in vitro by substoichiometric concentrations of tubulin-colchicine complex, *Biochemistry 34*, 9921−9929.
44. Jordan, M. A., Wendell, K., Gardiner, S., Derry, W. B., Copp, H., and Wilson, L. (1996) Mitotic block in HeLa cells by low concentrations of paclitaxel (taxol) results in abnormal mitotic exit and apoptotic cell death, *Cancer Res. 56*, 816−825.
45. Lin, H. L., Chang, Y. F., Lui, T. Y., Wu, C. W., and Chi, C. W. (1998) Submicromolar paclitaxel induces apoptosis in human gastric cancer cells at early G1 phase, *Anticancer Res. 18*, 3443−3449.
46. Abal, M., Andreu, J. M., and Barasoain, T. (2003) Taxanes: microtubule and centrosome targets and cell cycle dependent mechanisms of action, *Curr. Cancer Drug Targets 3*, 193−203.
47. Boise, L. H., Ganzalel-Garcia, M., Postema, C. E., Ding, L., Lindsten, T., Turka, L. A., Mao, X., Numez, G., and Thompson, C. B. (1993) Bcl-x1, a bcl-2 related gene that functions as a dominant regulator of apoptotic cell death, *Cell 74*, 597−608.
48. Haldar, S., Basu, A., and Croce, C. M. (1997) Bcl-2 is the guardian of microtubule integrity, *Cancer Res. 57*, 229−233.
49. Blagoskonny, M. V. (2001) Unwinding the loop of bcl-2 phosphorylation. *Leukemia 15*, 869−874.
50. Scatena, C. D., Stewart, Z. A., Mays, D., Tang, L. J., Keefer, C. J., Leach, S. D., and Pietenpol, J. A. (1998) Mitotic phosphorylation of bcl-2 during normal cell cycle progression and taxol-induced growth arrest, *J. Biol. Chem. 273*, 30777−30784.
51. Basu, A., and Haldar, S. (1998) Microtubule-damaging drugs triggered bcl2 phosphorylation- requirement of phosphorylation on both serine-70 and serine-87 residues of bcl2 protein, *Int. J. Oncol. 13*, 659−664.
52. Lanni, J. S., and Jacks, T. (1998) Characterization of the p53-dependent post mitotic checkpoint following spindle disruption, *Mol. Cell. Biol. 18*, 1055−1064.
53. Giannakakou, P., Nakauo, M., Nicolaou, K. C., O'Brate, A., Yu, J., Blagosklonny, M. V., Greber, U. F., and Fojo, T. (2002) Enhanced microtubule dependent trafficking and p53 nuclear accumulation by suppression of microtubule dynamics, *Proc. Natl. Acad. Sci. U.S.A. 99*, 10855−10860.
54. Lanni, J. S., Lowe, S. W., Licitra, E. J., Liu, J. O., and Jacks, T. (1997) P53-independent apoptosis induced by paclitaxel through an indirect mechanism, *Proc. Natl. Acad. Sci. U.S.A. 94*, 9679−9683.
55. Woods, C. M., Zhu, J., McQueney, P. A., Bollag, D., and Lazarides, E. (1995) Taxol-induced mitotic block triggers rapid onset of a p53-independent apoptotic pathway, *Mol. Med. (Tokyo, Jpn) 1*, 506−526.

BI0523409